Electrochemical and XPS investigations of cobalt in KOH solutions

K.M. ISMAIL and W.A. BADAWY
Chemistry Department, Faculty of Science, Cairo University, Giza, Egypt

Abstract

The electrochemical behaviour of cobalt in KOH solutions of different concentrations was studied. The effects of applied potential, temperature and the presence of aggressive Cl^- ions were investigated. Different electrochemical methods such as open-circuit potential measurements, polarisation techniques and electrochemical impedance spectroscopy (EIS) were used. The electrochemical behaviour of cobalt in naturally aerated KOH solutions is characterized by three different regions according to the alkali concentration. Corrosion behaviour was observed at high concentrations (0.3–1.0 M); passivation at lower concentrations (0.01–0.05 M), and at intermediate concentrations (0.1–0.2 M) corrosion followed by passivation was recorded. The corrosion parameters (i_{corr}, E_{corr}, and R_{corr}) under various conditions were calculated. Equivalent-circuit models for the electrode–electrolyte interface under different conditions were proposed. The experimental impedance data were fitted to theoretical data according to the proposed models. The relevance of the proposed models to the corrosion–passivation phenomena occurring at the electrode–solution interface was discussed. The electrochemical experimental results and discussions were supported by surface analytical techniques.

1. Introduction

Cobalt and its alloys have many important industrial applications such as cobalt-base superalloys, magnetic recording media, antiwear materials and surgical applications. Nevertheless sporadic work has been published concerning the electrochemical behaviour of cobalt in alkaline solutions [1–7]. Grube [1] and El-Wakkad and Hickling [2] found three potential arrests in galvanostatic transients of anodic oxidation of cobalt in alkaline solutions. Although Grube attributed these to the formation of Co_3O_4, Co_2O_3 and CoO_2, El-Wakkad and Hickling described them as corresponding to CoO, Co_2O_3 and CoO_2. Using cyclic voltammetry, Behl and Toni [3] and Jayaraman et al. [4] have suggested that the oxidation of cobalt results in the formation of $Co(OH)_2$ which is oxidised subsequently at more positive potentials to Co_3O_4 and CoOOH. Further, Behl and Toni have suggested that the passivation of cobalt is due to the formation of a CoO under film at the metal surface.

Recently, Badawy et al. [8, 9] studied the corrosion and passivation behaviour of cobalt in aqueous solutions of different pH. The metal was found to be covered by a native passive film which consists mainly of cobalt oxide (CoO) and/or hydrated cobalt oxide (CoO · H_2O) and is unstable in acidic solutions. In neutral solutions, stabilization of CoO and $Co(OH)_2$ takes place and in basic solutions the $Co(OH)_2$ passive film undergoes further oxidation to Co(III) compounds (CoOOH and/or Co_3O_4) depending on the electrode potential and the pH of the medium.

The present work is an investigation of the electrochemical behaviour of cobalt in KOH solutions of different concentrations intended to clarify the mechanism of the corrosion and passivation processes taking place at the electrode–electrolyte interface in basic solutions. The effects of applied potential, temperature, and the presence of aggressive Cl^- ions on the behaviour of this metal were studied. In this respect, different electrochemical techniques (e.g., open-circuit potential measurements, polarization techniques and electrochemical impedance spectroscopy (EIS)) were used. The electrochemical measurements were confirmed by surface analytical techniques, for example, X-ray photoelectron spectroscopy (XPS) and scanning electron microscopy (SEM).

2. Experimental details

The working electrode was made from spectroscopically pure cobalt rod, mounted in a glass tube of appropriate diameter by two-component epoxy resin leaving a specified circular surface area (0.32 cm^2) to contact the solution. A stout copper wire was employed as the electrical contact. The solutions were prepared from analytical grade reagents and triple-distilled water. Prior to each experiment, the working electrode was

mechanically polished using successive grades emery papers down to 1000 grit. The electrode was rubbed with a smooth polishing cloth, washed with triple distilled water and transferred quickly to the electrolytic cell containing a fresh KOH solution. The cell was a three-electrode all glass double walled cell, with a platinum counter electrode and a silver chloride reference electrode.

The open-circuit potential of cobalt was recorded from the moment of electrode immersion in the test solution until it reached steady state and up to 75 min using a high impedance digital multimeter. The electrochemical impedance investigations and the polarisation measurements were carried out using IM5d system (Zahner Elektrik GmbH, Kronach, Germany). The excitation amplitude was 10 mV peak-to-peak in a frequency domain 10^{-2}–10^5 Hz. Potential and current control in the cell were achieved using the same system. Except otherwise stated, all experiments were carried out at constant temperature of 25 ± 0.1 °C using a water thermostat with the double walled cell. The potentials were measured against and referred to the Ag/AgCl/Cl$^-$ (3 M KCl) reference electrode ($E^\circ_{Ag/AgCl/Cl^-} = 0.197$ V vs NHE). All cyclic voltammetry measurements were carried out using a scan rate of 10 mV s^{-1} after polarising the cobalt electrode at -1.2 V for 10 min. It was reported that the polarization of the cobalt surface at -1.2 V vs NHE for 10 s leads to the reduction of any native oxide as was confirmed by Mössbauer spectroscopy [6]. For the calculation of the Tafel constants, the potentiodynamic measurements were conducted at a scan rate 0.5 mV s^{-1} to achieve conditions close to the steady state. Details of the experimental procedures are described elsewhere [10, 11].

The composition and the structure of the passive film formed on the metal surface were examined by X-ray photoelectron spectroscopy (XPS) and scanning electron microscopy (SEM). For this purpose, special cobalt discs with the same surface area were prepared. The discs were pretreated as described before. X-ray photoelectron spectra were measured by VG ESCA LAB 200 scientific instrument (8 eV resolution and 8 mcps sensitivity for clean surface) based on irradiation of a specimen in ultrahigh vacuum (10^{-10}–10^{-11} torr) with Mg/Al dual anode X-ray source (1200–1500 eV). For the cobalt surface, AlK$_\alpha$ line (1486.6 eV) was used for X-ray excitation. The specimen was pretreated with reactive gases under high pressure and at temperature up to 300 °C. For surface sputtering, argon ion bombardment was required to determine the thickness of the passive film. An AG 21 argon gun with 10 keV energy source and 1 μA current was used to detect the depth profiling.

3. Results and discussion

3.1. Open circuit potential measurements

The open-circuit potential of Co was followed over a period of 75–90 min in naturally aerated KOH solutions of different concentrations. Typical results in 0.01–1.0 M KOH solutions are presented in Figure 1. The steady state is reached within different periods of time depending on the alkali concentration. In solutions of low concentration ($\leqslant 0.05$ M), the open-circuit potential of the metal becomes more noble until it reaches the steady state within $\sim$20 min. This indicates that a passivation process occurs at the metal surface from the moment of electrode immersion. In solutions of high concentration ($\geqslant 0.3$ M) the electrode potential becomes more negative and reaches steady state in less than 5 min, which indicates the presence of a continuous steady corrosion process. In solutions with intermediate concentration (0.1–0.2 M) the potential shifts towards more negative values within the first few minutes then passes through two arrests. The first arrest occurs at a steady state value of about -790 mV which extends over 25 and 60 min for 0.1 and 0.2 M KOH solutions, respectively. The potential then jumps to the second arrest which occurs at about -290 mV. At intermediate alkali concentrations a corrosion–passivation process is occurring at the electrode–electrolyte interface. At the moment of electrode immersion corrosion is the predominant process and after a certain period the passivation process dominates, leading to the ennobling of the electrode potential.

3.2. Potentiodynamic and EIS measurements

The cyclic voltammograms of cobalt were recorded at a scan rate of 10 mV s^{-1} in KOH solutions of different concentration. A typical cyclic voltammogram for cobalt in naturally aerated ((a) 0.05 M and (b) 0.2 M) KOH solution at 25 °C is shown in Figure 2. On the anodic sweep, oxidation commences at about -0.9 V.
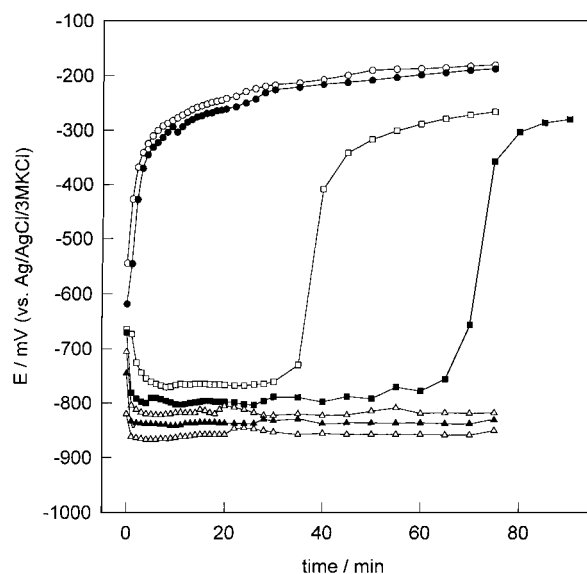

Fig. 1. Variation of the cobalt electrode potential with time in naturally aerated KOH solution of different concentrations at 25 °C. Key: (○) 0.1, (●) 0.05, (□) 0.1, (■) 0.2, (△) 0.3, (▲) 0.5 and (△) 1.0 M.
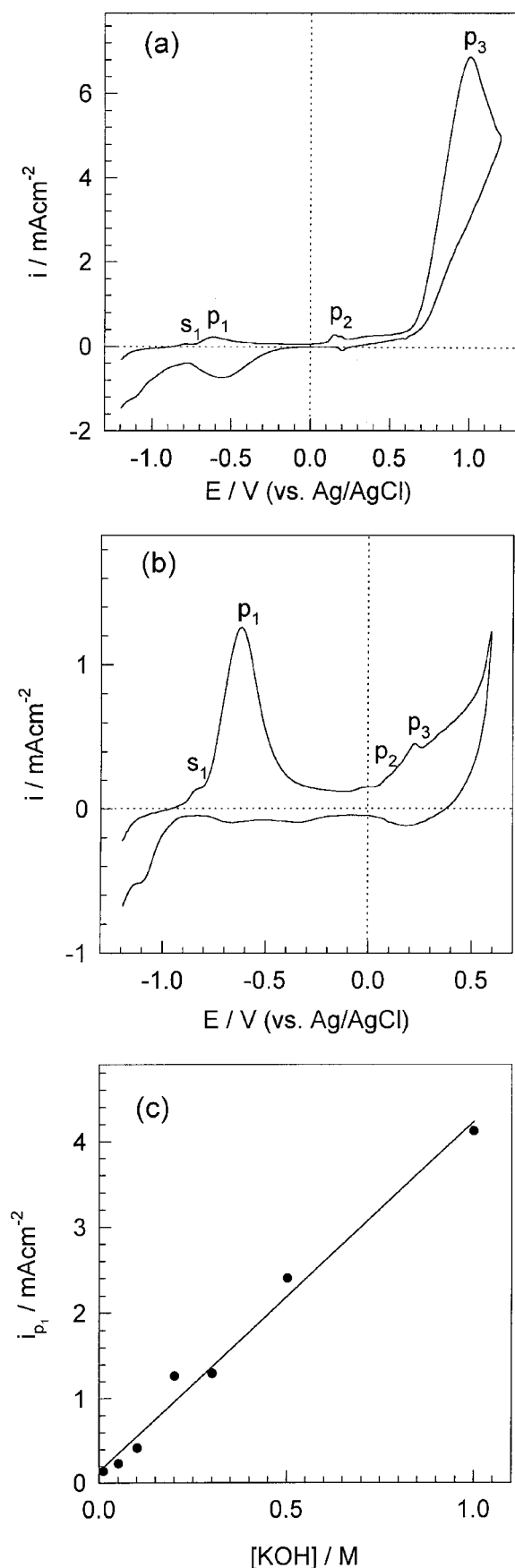
Fig. 2. Cyclic voltammograms of cobalt in naturally aerated KOH solution of different concentrations at 25 °C and a scan rate of 10 mV s^{-1}; (a) 0.05 M, (b) 0.2 M, (c) i_p vs [KOH] (the peak current, i_p, of the first peak (ii) against the concentration of the alkali).
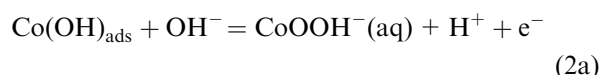
All the cyclic voltammograms exhibit a clear shoulder (s$_1$) at about −0.8 V, which can be attributed to the formation of Co(OH)$_{ads}$ at the electrode surface [12] via the reaction

$$Co + OH^- = Co(OH)_{ads} + e^- \tag{1}$$
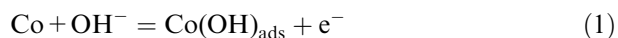
The first anodic peak (p$_1$) appears as a minor peak in dilute KOH solutions ($\leqslant$0.1 M) (cf. Figure 2(a)), and as a major peak at about −0.6 V in solutions of higher KOH concentrations (0.2–1.0 M) (cf. Figure 2(b)). The presence of the major peak indicates the high reactivity of the metal at higher KOH concentrations. It can be attributed to a combination of a dissolution–passivation processes [13] described as follows:

(a) *Dissolution.* That is, the dissolution of the adsorbed layer of Co(OH)$_{ads}$ and/or the metal itself according to the following:
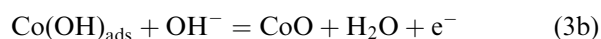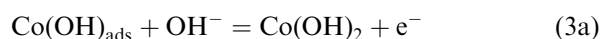
(i) from the covered area

$$Co(OH)_{ads} + OH^- = CoOOH^-(aq) + H^+ + e^- \tag{2a}$$

(ii) from the bare surface
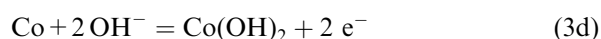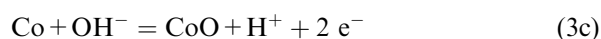
$$Co + 2OH^- = CoOOH^-(aq) + H^+ + 2e^- \tag{2b}$$
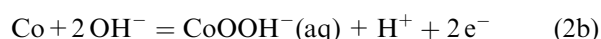
(b) *Passivation.* That is, formation of a stable passive film of CoO or a hydrated oxide Co(OH)$_2$, according to the following:

(i) from the adsorbed film:

$$Co(OH)_{ads} + OH^- = Co(OH)_2 + e^- \tag{3a}$$

$$Co(OH)_{ads} + OH^- = CoO + H_2O + e^- \tag{3b}$$

(ii) from the bare surface:

$$Co + OH^- = CoO + H^+ + 2 e^- \tag{3c}$$

$$Co + 2OH^- = Co(OH)_2 + 2 e^- \tag{3d}$$

The height of the first anodic peak is concentration dependent, that is, the anodic dissolution current increases as the concentration of OH$^-$ ions increases (cf. Figure 2(c)). Another minor anodic peak (p$_2$) is observed at about +0.2 V in solutions with high and low alkali concentration. This peak can be attributed to the conversion of the outer layer of the oxide film, largely Co(OH)$_2$, at the oxide–solution interface to Co(II)/Co(III) oxide [3], according to

$$Co(OH)_2 + OH^- = CoOOH + H_2O + e^- \tag{4a}$$

$$3\,Co(OH)_2 + 2\,OH^- = Co_3O_4 + 4\,H_2O + 2\,e^- \tag{4b}$$
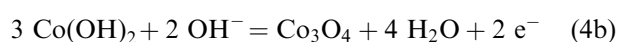
A third anodic peak appears (p$_3$) at about +0.25 V at concentrations ($\geqslant$0.2 M). This peak can be attributed to the formation of Co(III) oxide, Co$_2$O$_3$, namely,
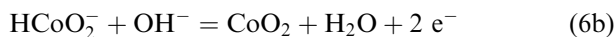
$$2\,Co(OH)_2 + 2\,OH^- = Co_2O_3 + 3\,H_2O + 2\,e^- \tag{5}$$
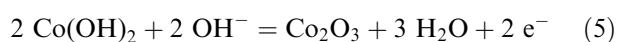
At lower concentrations ($\leqslant 0.1$ M) the third anodic peak (p_3) appears at about $+1.0$ V just prior to the oxygen evolution and can be attributed to the dissolution–precipitation processes according to

(a) *Dissolution*:

$$Co + CoOOH + 3 \, OH^- = 2 \, HCoO_2^- + H_2O + e^-$$

(6a)
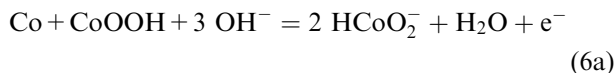
(b) *Precipitation of CoO$_2$, namely*,

$$HCoO_2^- + OH^- = CoO_2 + H_2O + 2 \, e^-$$

(6b)

This oxide film contributes little protection to the metal surface as indicated by the high anodic current (cf. Figure 2(a)). On reversing the sweep a small cathodic current was recorded. The minor and relatively broad cathodic peaks indicate that the passivating film formed on cobalt in KOH solutions is not easily reduced. The incomplete reversibility of the electroreduction steps and the high rate of dissolution of the surface substances explain the relatively small cathodic currents [6].

The impedance data recorded after 75 min of electrode immersion in KOH solutions of different concentrations are presented in Figure 3. The Bode plots show resistive regions at the high and low frequencies and a capacitive region at the intermediate frequencies. The impedance values were found to depend on KOH concentration. The impedance spectra obtained experimentally were analysed using EQUIVALENT CIRCUIT software [14] and three equivalent circuits (cf. Figure 4) from which the impedance parameters were calculated. Sometimes simple elements such as capacitors, resistors, and diffusion related elements are not sufficient to represent the measured impedance data [15]. The impedance data for cobalt in KOH solutions
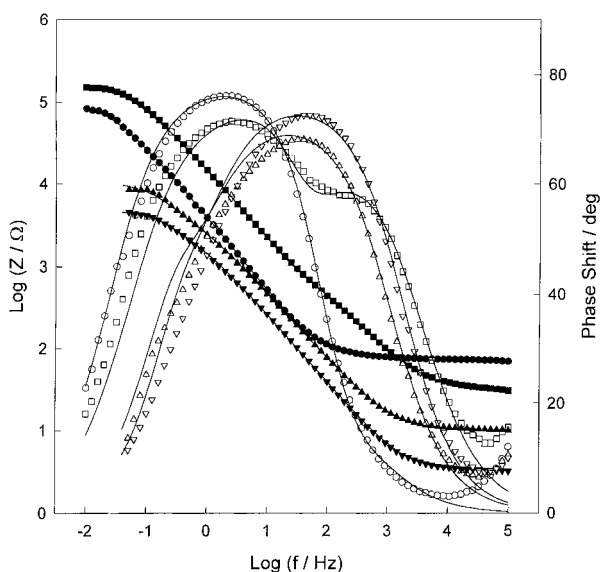
of different concentrations under open circuit potential conditions were analysed using the equivalent circuit model illustrated in Figure 4(a). The electrode impedance is represented by the impedance of a constant phase element, Z_{CPE}, in parallel with a resistor, representing the passive film resistance, R_{pf}, in parallel with a capacitor and resistor, representing the double layer capacitance, C_{dl}, and the charge transfer resistance, R_{ct}, respectively. The solution resistance is represented by a resistor, R_s, in series with the above parallel combination. The Z_{CPE} impedance is described as: $Z_{CPE} = 1/Y(j\omega)^n$ where ω is the angular frequency in rad/s, Y is the admittance and n is an empirical exponent which varies between 1 for a perfect capacitor, and 0 for a perfect resistor. A value of n less than one would represent a somewhat imperfect capacitor and is generally thought to arise from the presence of heterogeneities both laterally and within the passive film [16].

Using the equivalent circuit shown in Figure 4(a) the equivalent circuit parameters for cobalt after 75 min of electrode immersion in solutions of different concentrations are presented in Table 1. The surface of the cobalt electrode in high concentrations of KOH solution was found to be more heterogeneous ($n \approx 0.67$) than that in
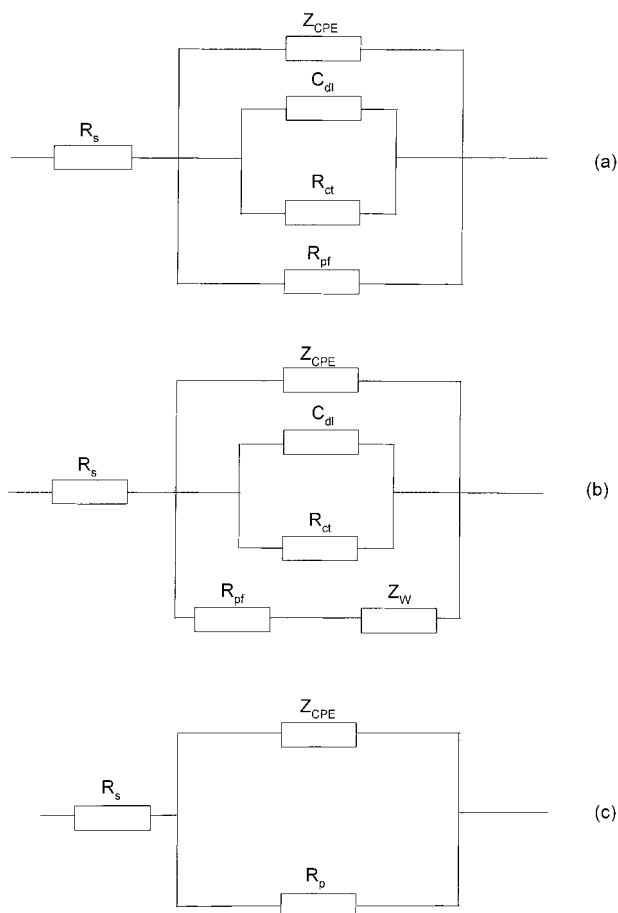
Fig. 4. Equivalent circuits used in the fitting of the impedance data of cobalt at different conditions; R_s = solution resistance, R_{pf} = passive film resistance, R_{ct} = charge transfer resistance, Z_{CPE} = impedance of constant phase element, C_{dl} = double layer capacitance, and Z_w = Warburg impedance.

Fig. 3. Bode plots of cobalt after 75 min of electrode immersion in naturally aerated KOH solution of different concentrations at 25 °C. Key: (●) 0.05, (■) 0.1, (▲) 0.3 and (▼) 1.0 M. (—) Simulated.

Table 1. Equivalent circuit parameters for Co after 75 min of electrode immersion in naturally aerated solutions of KOH of different concentrations at 25 °C

KOH/M	R_s/Ω	Y/Ω^{-1}	n	R_{ct}/Ω	$C_{dl}/\mu F\ cm^{-2}$	$R_{pf}/k\Omega$
0.01	319	2.2×10^{-5}	0.84	210	21.5	163
0.05	71	4.1×10^{-5}	0.83	45	35	103
0.1	31	1.3×10^{-5}	0.78	2194	5.9	199
0.2	15	1.5×10^{-5}	0.77	126	1.8	224
0.3	9	8.7×10^{-5}	0.71	5.2	25.4	11.7
0.5	5	14.8×10^{-5}	0.68	2.9	4.9	6.5
1.0	3	14.6×10^{-5}	0.67	1.7	71.2	6.7

low concentrations ($n \approx 0.84$). Such heterogeneity is due to the corrosion of the electrode surface in high concentrations of KOH solution as observed from open circuit potential measurements of cobalt, that is, the shift of the open-circuit potential towards more negative potential (cf. Figure 1).

To investigate the corrosion and passivation processes occurring at the electrode surface, it was important to investigate the impedance characteristics of the Co electrode under anodic polarisation. Therefore, a constant potential was applied to the cobalt electrode in 0.05 M KOH until a steady state was reached and then the impedance spectra were recorded. The results of these measurements are presented as Bode plots in Figure 5. Although the electrochemical impedance was measured down to very low frequencies (10 mHz), the Bode plots do not show a resistive region (horizontal line and a phase angle $\approx 0°$) at these frequencies. The data analysis at different potentials is represented in Table 2. The impedance at different potentials was analysed using the equivalent circuit shown in Figure 4(b) where a Warburg impedance, Z_w, was introduced to account for a diffusion process within the interfacial layer. The impedance data under constant
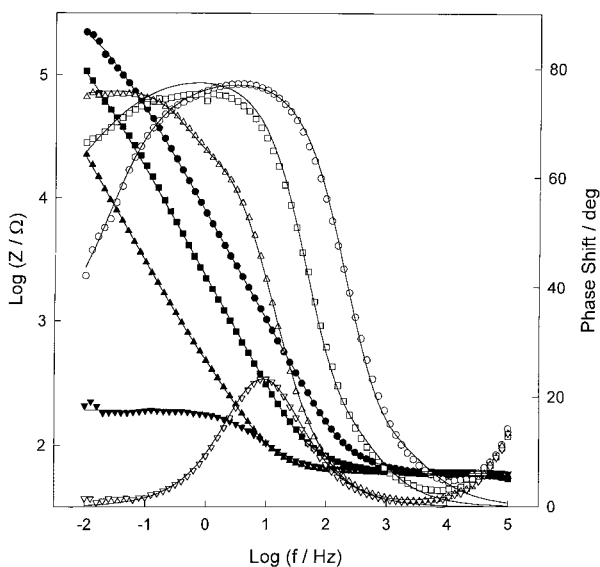

Fig. 5. Bode plots of cobalt in naturally aerated 0.05 M KOH solution at different applied potentials. Key: (●) −100, (■) +100, (▲) +500 and (▼) +700 mV. (—) Simulated.

potential show a diffusion contribution which should be accounted for, and the equivalent circuit model of Figure 4(b) was found to give the best fitting for these data. Such diffusion process may indicate reversible dissolution process, that is, the passive film formation under potentiostatic condition proceed through a dissolution–precipitation mechanism [17]. The impedance measurements show a passivation behaviour for applied potentials from −100 up to +500 mV, where the passive film formed on cobalt shows high resistance ranges from 207 to 2100 kΩ. For an applied potential $\geqslant +700$ mV the simple Randles circuit (Figure 4(c)) was found to be satisfactory for fitting the data. The calculated resistance at +700 mV was found to be low (131 Ω), indicating significant anodic dissolution at this potential.

3.3. *X-ray photoelectron spectroscopy (XPS)*

The results of the electrochemical measurements were confirmed by XPS. The XP survey spectrum of the mechanically polished cobalt surface shows the following peaks; the Co peaks (Co 2p1 at 797.7 eV and 2p3 at 781.9 eV), clear oxygen peak (O 1s at 532.2 eV) and a small carbon peak (C 1s at 285.6 eV, as a residual of the vapours of the oil pumps) [18, 19]. The clear oxygen peak indicates that the cobalt surface is covered by a native oxide film. This was confirmed by surface sputtering with argon ion bombardment, which has shown that the cobalt peaks were shifted towards lower binding energy values where they match those of standard metallic cobalt [19, 20] (Co 2p1 at 795.0 eV and Co 2p3 at 777.9 eV). Also, the oxygen peak was diminished after surface sputtering. The native oxide film consists of α-Co(OH)$_2$ and CoO as confirmed by the matching of the cobalt peaks of the working electrode after polishing and contacting the normal atmosphere and those of standard α-Co(OH)$_2$ and CoO.

The immersion of the working electrode in the alkali solution has led to a XP spectrum identical with that of CoOOH where the Co 2p1 at 798.4 eV, Co 2p3 at 782.4 eV and O 1s at 532.7 eV peaks were recorded. After surface sputtering with argon ion bombardment for 20 min, which is equivalent to 4 nm of the surface film thickness [18, 21, 22], the Co 2p1 broadens, showing two peaks at 803.2 and 796.6 eV and the Co 2p3 shows also two peaks at 787.0 and 780.4 eV as shown in Figure 6. At the same time the O 1s peak broadens

Table 2. Equivalent circuit parameters for Co electrode in naturally aerated solutions of 0.05 M KOH at different applied potentials at 25 °C

E_{app} /mV	R_s /Ω	Y /Ω^{-1}	n	R_{ct} /Ω	C_{dl} /$\mu F\ cm^{-2}$	R_{pf} /kΩ	W /Ω^{-1}
−100	56	2.2×10^{-5}	0.83	42.5	15.6	263	32×10^{-6}
+100	57	7×10^{-5}	0.84	65	54.1	207	20×10^{-6}
+300	59	0.4×10^{-5}	0.81	66.9	29.8	2100	9×10^{-6}
+500	59	0.5×10^{-5}	0.84	4490	173	650	1×10^{-6}
+700	61	52×10^{-5}	0.81	131	–	–	–

showing two peaks at 532.1 and 530.0 eV. This means that after removal of 4 nm of the surface layer, the surface is still covered by a passive film which has two cobalt–oxygen contributions. These two contributions match the α-Co(OH)$_2$ and CoO as recorded in the comparative XP survey spectra, that is, the inner oxide layer has both OH$^-$ and O^{2-} species.

The XPS data confirm that the surface film formed on Co in alkali solution consists of two layers. The inner layer consists of α-Co(OH)$_2$ and CoO which is identical with the native oxide film and the outer layer consists of the Co(III) as was confirmed by XPS survey spectra. The presence of the Co(III) compound is responsible for the shift in the steady state potential towards more positive values as shown in Figure 1. The formation of the relatively thick (>4 nm) passive film on the cobalt surface in the alkali solution is responsible for its smooth appearance as confirmed by SEM (not shown) and even the naked eye. It must be pointed out that the electrode surface after contacting the atmosphere and the sputtered surface after long immersion in the alkali solution acquires a bluish colour [20] similar to that of α-Co(OH)$_2$.

3.4. Effect of temperature on the corrosion rate of cobalt

To calculate the activation energy of the corrosion process taking place at the electrode/electrolyte interface, the effect of temperature was investigated in naturally aerated 0.05 M KOH solution. From potentiodynamic Tafel polarization data obtained at quasi-stationary conditions, the values of the corrosion parameters, that is, corrosion current density, i_{corr}, corrosion potential, E_{corr}, and corrosion resistance, R_{corr}, were calculated and are presented in Table 3. The calculated Tafel slopes are in the range 89–200 mV decade^{-1} which indicates that the corrosion process is under activation control. In general, the corrosion current density, i_{corr}, increases with increasing temperature, and the process obeys the familiar [23] Arrhenius equation

$$\frac{d \log i_{corr}}{dT} = \frac{E_a}{RT^2} \tag{7}$$

where E_a is the molar activation energy of the process occurring at the electrode–electrolyte interface and R is the gas constant (8.314 J mol^{-1} K^{-1}). Figure 7 presents the Arrhenius plot of log i_{corr} vs $1/T$. The calculated value of E_a was found to be 15.4 kJ mol^{-1}. This low value of the activation energy (<40 kJ mol^{-1}) indicates that the rate determining step for the dissolution of cobalt is a one electron transfer process [9, 24]. Thus the rate determining dissolution step can be represented by Equation 2.

Table 3. Corrosion parameters of Co in naturally aerated solution of 0.05 M KOH at different temperatures

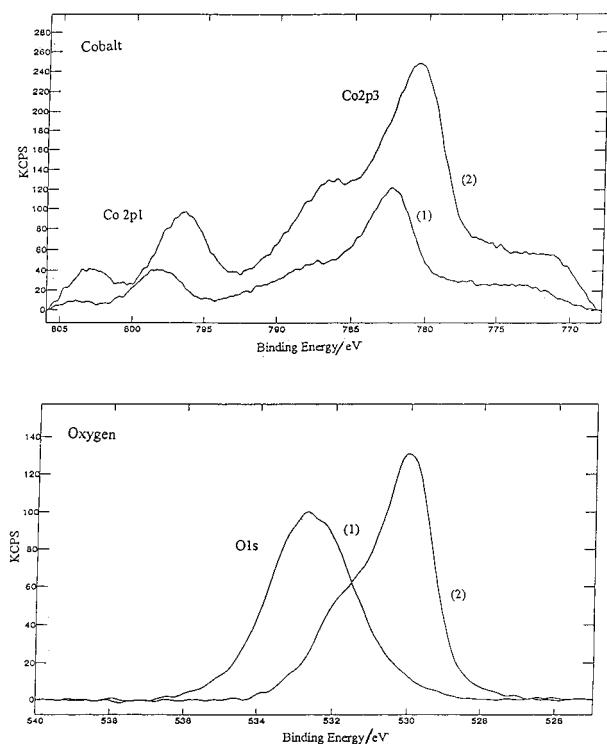| T /°C	E_{corr} /mV	R_{corr} /kΩ	i_{corr} /μA cm^{-2}	b_a /mV decade^{-1}	b_c /mV decade^{-1}
15	−360	93	0.5	100	200
25	−269	79	0.9	122	190
35	−222	52	1.6	114	138
45	−218	36	2.4	150	100
55	−208	36	3.1	89	98
65	−159	–	4.9	–	92

Fig. 6. Depth profiling of cobalt surface after immersion in alkali solution (the Co 2p1 and 2p3 peaks and the O 1s peak) (1) before sputtering, (2) after 20 min sputtering by argon ion bombardment.
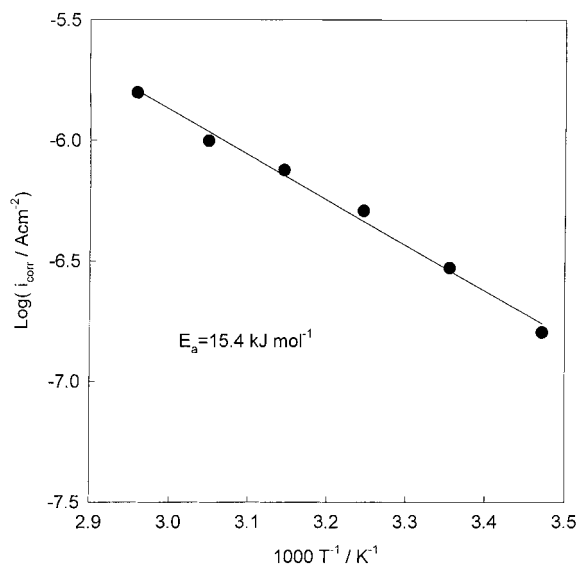

Fig. 7. Arrhenius plot of the corrosion of cobalt in naturally aerated 0.05 M KOH solution.

3.5. *Effect of chloride ions*

The effect of chloride ions on the electrochemical behaviour of cobalt in naturally aerated 0.05 M KOH solution was investigated. The results of open-circuit potential measurement showed that at relatively high concentrations of chloride ions (>0.05 M), the steady state potential of the cobalt electrode becomes more negative with increase in Cl⁻ concentration. This indicates that active corrosion occurs at the metal surface. Below a certain concentration (<0.05 M) chloride showed no significant effect (cf. Figure 8).

The effect of chloride ions was also investigated by EIS. The impedance results are presented as Bode plots in Figure 9. These data were analysed using the equivalent circuit shown in Figure 4(a) and the calculated parameters are displayed in Table 4. In the presence of 0.05 M NaCl the passive film resistance was 91 kΩ compared to 103 kΩ in Cl⁻ free alkali solution. At a concentration of 0.6 M NaCl in the same solution the recorded passive film resistance decreased to 24 kΩ. The decrease in the passive film resistance can be attributed to the dissolution of the passive film at high Cl⁻ concentration. Fitting of the experimental impedance data to the equivalent circuit model of Figure 4(a) gave a value of 0.86 for the factor *n*, which shows that Cl⁻ does not change the passive film heterogeneity and the double layer capacitance was found to be in the typical range 25–42 μF cm⁻².

The electrochemical impedance data were also confirmed by the polarization technique. The corrosion parameters of the cobalt electrode in naturally aerated 0.05 M KOH containing different concentrations of Cl⁻ were calculated and are presented in Table 5. The corrosion current was found to increase with increasing chloride ion concentration. The results in Table 5 show
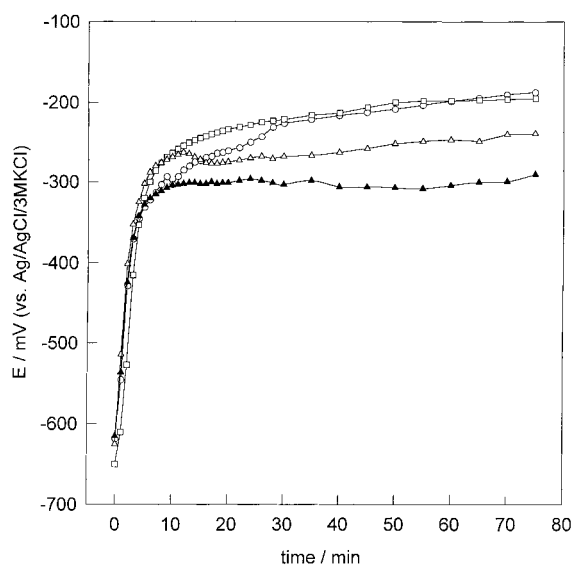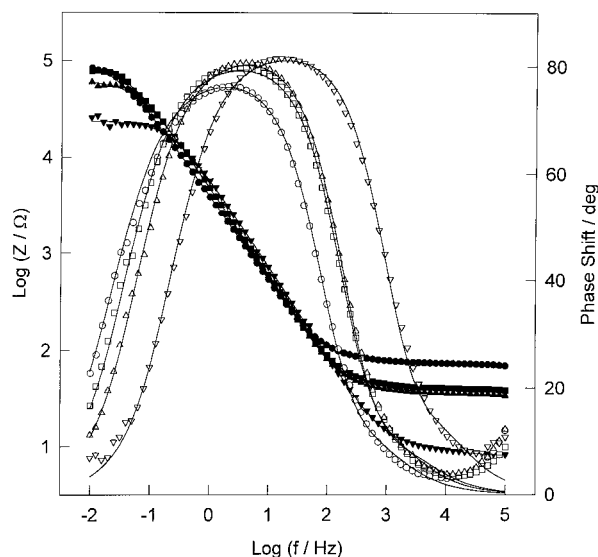

Fig. 9. Bode plots of cobalt after 75 min of electrode immersion in naturally aerated 0.05 M KOH solution containing different Cl⁻ ion concentrations at 25 °C. Key for NaCl concentration: (●) 0.00, (■) 0.05, (▲) 0.1 and (▼) 0.6 M. (—) Simulated.

that the Tafel slopes are in the range of 72–146 mV decade⁻¹ which indicates that the corrosion of cobalt in the presence of Cl⁻ is under activation control and that the mechanism of the corrosion process is unchanged.

Above a certain concentration, the corrosion current density was found to change exponentially with chloride ion concentration. This means that $\log i_{corr}$ is a linear function of the concentration of Cl⁻ at concentrations $\geqslant 0.05$ M (cf. Figure 10). This linear relation can be formulated mathematically as

$$\log i_{corr} = \log k + \alpha[Cl^-] \tag{8}$$

Fig. 8. Variation of the cobalt electrode potential with time in naturally aerated 0.05 M KOH solution containing different chloride ion concentrations at 25 °C. Key for 0.05 M KOH + *x* M NaCl: (○) *x* = 0.00, (□) *x* = 0.05, (△) *x* = 0.3 and (▲) *x* = 0.6.

Table 4. Equivalent circuit parameters for Co electrode in naturally aerated solutions of 0.05 M KOH containing different Cl⁻ ion concentrations at 25 °C

NaCl/M	R_s/Ω	Y/Ω^{-1}	n	R_{ct}/Ω	C_{dl}/μF cm⁻²	$R_{pf}/$kΩ
0.01	54	3.4×10^{-5}	0.84	19	41.6	94
0.05	39	3.1×10^{-5}	0.86	23	30.6	91
0.1	35	2.6×10^{-5}	0.86	14	39.7	62
0.3	15	2.5×10^{-5}	0.87	15	24.9	44
0.6	8	2.2×10^{-5}	0.87	6.1	27.9	24

Table 5. Corrosion parameters of Co in naturally aerated 0.05 M KOH solution containing different Cl⁻ ion concentrations at 25 °C

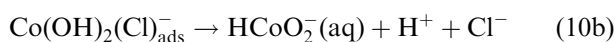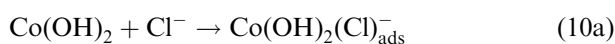| NaCl /M	E_{corr} /mV	R_{corr} /kΩ	i_{corr} /μA cm⁻²	b_a /mV decade⁻¹	b_c /mV decade⁻¹
0.00	−268	79	1	72	112
0.01	−275	69	1.1	83	111
0.05	−295	64	1.2	78	110
0.1	−304	61	1.3	96	146
0.3	−300	53	1.5	85	85
0.6	−291	49	1.9	96	134
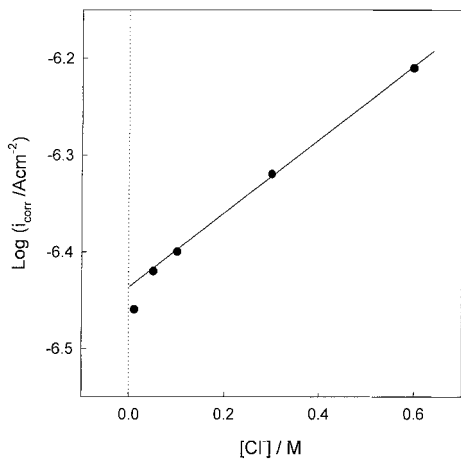
Fig. 10. Variation of the rate of corrosion of Co in naturally aerated 0.05 M KOH solution as a function of Cl^- ion concentrations at 25 °C.

where k is a constant which can be obtained from the intercept of the linear, $\log i_{corr}$ vs $[Cl^-]$ relation and α is its slope, $d \log i_{corr}/d[Cl^-]$. The values of k and α were calculated and found to be 3.7×10^{-7} A · cm^{-2} and 0.4, respectively. The increase in the rate of corrosion as a function of chloride ion concentration can be attributed to the interaction of Cl^- with the barrier layer at the metal surface. It seems that the chloride ions attack the outermost layer and do not penetrate the surface, as confirmed by XPS measurements.

The XP spectra of the electrode immersed in chloride solution of low concentration $\leqslant 0.05$ M are similar to those of chloride free solutions. After immersion in alkali solutions containing $[Cl^-] \geqslant 0.35$ M the Co and O peaks related to the Co(III) compound disappear and those corresponding to CoO and α-Co(OH)$_2$ are still present. This means that the increase in Cl^- concentration leads to the dissolution of the outer Co(III) oxide layer and the rate of corrosion increases. The XP spectra showed no chloride peaks, which means that unlike other surface films [26, 27] the chloride ions do not penetrate the oxide film but enhance the rate of dissolution of the outer layer of Co(III). The mechanism of the dissolution process can be represented by

$$CoOOH + Cl^- \rightarrow CoOOH(Cl)^-_{ads} \quad (9a)$$

$$CoOOH(Cl)^-_{ads} \rightarrow CoO_2^-(aq) + H^+ + Cl^- \quad (9b)$$
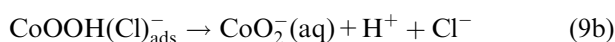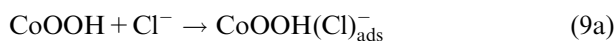
Long time immersion of the electrode in the chloride containing solution leads to the dissolution of α-Co(OH)$_2$ according to the following:

$$Co(OH)_2 + Cl^- \rightarrow Co(OH)_2(Cl)^-_{ads} \quad (10a)$$

$$Co(OH)_2(Cl)^-_{ads} \rightarrow HCoO_2^-(aq) + H^+ + Cl^- \quad (10b)$$

It must be stated, however, that such an increase in the corrosion rate was true only in the presence of relatively high concentrations of chloride ions ($[Cl^-] \geqslant 0.05$ M). At lower concentration no significant increase in the corrosion rate was recorded. This indicates that there is a critical concentration below which no significant effect of chloride ions can be considered. The critical concentration of Cl^- was found to be in the range of 0.05 M.

4. Conclusions

(i) Cobalt exhibits three different electrochemical behaviours depending on KOH concentration: (i) corrosion, (ii) corrosion followed by passivation, and (iii) passivation.
(ii) The passive film formed on cobalt surface in alkali solution consists of two layers: the inner layer is α-Co(OH)$_2$ and CoO and the outer layer consists of Co(III) species (CoOOH).
(iii) Although the activation energy of the corrosion process for cobalt in KOH solution is low (15.4 kJ mol^{-1}), the relatively high corrosion resistance of the metal is due to the passive film formed on its surface.
(iv) The presence of chloride ions decreases the resistance of the passive film and, below a critical concentration ($[Cl^-] \leqslant 0.05$ M), chloride ions have no significant effect on the corrosion behaviour.
(v) The chloride ions do not penetrate the passive film but enhance its dissolution.

References

1. G. Grube and O. Feucht, *Z. Elektrochem.* **28** (1922) 568. G. Grube, *Z. Elektrochem.* **33** (1927) 389.
2. S.E.S. El-Wakkad and H. Hickling, *Trans. Faraday Soc.* **46** (1950) 1820.
3. W.K. Behl and J.E. Toni, *J. Electroanal. Chem.* **31** (1971) 63.
4. T.R. Jayaraman, V.K. Venkatesan and H.V.K. Udupa, *Electrochim. Acta* **20** (1975) 209.
5. N. Sato and T. Ohtsuka, *J. Electrochem. Soc.* **125** (1978) 1735.
6. I.M. Novoselsky and N.R. Menglisheva, *Electrochim. Acta* **29** (1984) 21.
7. S.S. Abd ElRehim, A.A. AL Basosi and M.M. Osman, *J. Electroanal. Chem.* **348** (1993) 99.
8. W.A. Badawy, F.M. Al-Kharafi and J.R. Al-Ajmi, *J. Appl. Electrochem.* **30** (2000) 63.
9. W.A. Badawy, F.M. Al-Kharafi and J.R. Al-Ajmi, *Br. Corr. J.* accepted.
10. W.A. Badawy, S.S. El-Egamy and Kh.M Ismail, *Br. Corr. J.* **28** (1993) 133.
11. W.A. Badawy, S.S. El-Egamy and A.S. El-Azab, *Corrosion* **53** (1997) 842.
12. L.D. Burke and M.M. Murphy, *J. Electrochem. Soc.* **138** (1991) 88.
13. L.D. Burke, M.E. Lyons and O.J. Murphy, *J. Electroanal. Chem.* **132** (1982) 247.
14. B.A. Boukamp, 'Equivalent Circuit', Version 4.55 (1996). Copyright B.A. Boukamp, University of Twente, The Netherlands (1993–96).
15. J.H. Wang, F.I. Wei and H.C. Shih, *Corrosion* **52** (1996) 24.
16. M. Drogowska, L. Bossard, H. Menard and A. Lasia, *Materials Science Forum* **192** (1995) 89.
17. R.D. Armstrong, *Corros. Sci.* **11** (1971) 693.

18. W.A. Badawy and F.M. Al-Kharafi and E.Y. Al-Hassan, *Corros. Prev. Control* **95** (1998) 8.
19. F.M. Al-Kharafi and W.A. Badawy, *Corrosion* **53** (1997) 68.
20. E. Adem, 'VG Scientific XPS Handbook', 1st edn (VG Scientific, East Grinstead, West Sussex RH 19 1UB, UK (1989).
21. F.M. Al-Kharafi and W.A. Badawy, *Bull. Electrochem.* **12** (1996) 505.
22. W.A. Badawy, F.M. Al-Kharafi and A.S. El-Azab, *Corros. Sci.* **41** (1999) 709.
23. P.W. Atkins, 'Physical Chemistry', 5th edn (Oxford University Press, Oxford, 1994), p. 877.
24. G.A. Wright, *J. Electrochem. Soc.* **114** (1967) 1263.
25. S.S. El-Egamy, A.S. El-Azab and W.A. Badawy, *Corrosion* **50** (1994) 468.
26. W.M. Carol and C.B. Berslin, *Br. Corr. J.* **26** (1991) 225.
27. W.A. Badawy and F.M. Al-Kharafi, 'Current Topics in Electrochemistry', Vol. 6 (1998), p. 33.